International Journal for Multidisciplinary Research (IJFMR)
E-ISSN: 2582-2160 ● Website: www.ijfmr.com ● Email: editor@ijfmr.com

Correlation between LST, NDVI and NDBI with Reference to Urban Sprawling – A Case Study of Shimla City

Sunil Jaswal[1], Paritosh Thakur[2]

[1]Assistant Professor/PO, Department of Environmental Science, Himachal Pradesh University, Summer Hill, Shimla.
[2]Researcher, Department of Environmental Science, Himachal Pradesh University, Summer Hill, Shimla.

Abstract
The present study aims to explain the impacts of urban expansion on land surface temperature and vegetation of Shimla city using integrated techniques of remote sensing (RS) and geographic information system (GIS). Remote sensing technique often analyses the thermal characteristics of any area. This study monitors the interrelationship of land surface temperature (LST) with two spectral indices (normalized difference vegetation index and normalized difference built-up index) in Shimla City of India using Landsat 8 satellite for summer season for the period 2014 to 2023. There is a synergetic relationship between urban expansion and LST. The result showed a linear correlation between increasing the built-up area and the higher Land Surface Temperature values while lower Land Surface Temperature was associated with vegetation cover which means that the there was a positive relationship between the normalized difference built-up index values and the Land Surface Temperature while the relation between the normalized difference vegetation index and Land Surface Temperature was inverse. These results provide an insight into the systematic planning of the urban environment in the study.

Keywords: Land surface temperature, remote sensing, normalized difference vegetation index, urban expansion, normalized difference built-up index.

1. Introduction

The world's cities are continuously growing in terms of population and physical expansion. The manner in which rural lands are developed for urban and suburban land use has become a matter of almost important for consideration. Removal of rural land-cover types, such as soil, water, vegetation and their replacement with common urban materials such as asphalt, concrete and metal, has significant environmental implications, including reduction in evapo-transpiration, promotion of more rapid surface runoff, increased storage and transfer of sensible heat along with reduction in air and water quality. These changes, in turn, can have negative effects on landscape aesthetics, energy efficiency, human health and quality of living in urban environments. In the last decade, researchersattention was increasingly drawn to local and regional climate under anthropogenic influences to understand the increasing change in the climate's driving factors. Bi-temporal characterization of land surface

temperature in relation to impervious surface area, NDVI and NDBI, using a sub-pixel image analysis has been studied by [15].[2] Carried out an investigation to assessed the relationship between land surface temperatures (LST) and changes of land cover (LC) for study area, by using Landsat TM/ETM+ data over the period from1990 to 2009.[9] calculated land surface emissivity by converting Landsat 8 Thermal Infrared Sensor (TIRS) and Operational Land Imager (OLI) band data to top-of-atmosphere spectral radiance using radiance rescaling factors. [7]did comparison of NDVI and NDBI as indicators of surface urban heat island effect in Landsat 8 imagery. Quantitative analysis of spatial distribution of land surface temperature (LST) in relation Ecohydrological, terrain and socio- economic factors based on Landsat data in mountainous area has been carried out by [3]. Land surface temperature (LST) is a direct impact of urbanization and a crucial factor in global climate and land cover changes [11]. Several studies have been reported on the retrieval of LST from Landsat imagery[13, 10, 14, 1, 4]**.**

[12]Identified spatial planning issues and analyse the urban sprawl through the use of spatial data from secondary and free sources of information. Like many other cities around the world, Shimla has experienced and facing the issue of urban sprawling which has been a significant concern over the years. Shimla city has witnessed a rapid increase in population along with surge in construction activities, leading to the encroachment of hillsides and the conversion of agricultural lands. This uncontrolled expansion has resulted in various environmental, social and infrastructural challenges.
The study investigates the impact of NDVI and NDBI on LST and the impact of increasing LST on climate change. It suggests that NDVI, NDBI change and LST should be correlated, except for meteorological data. Surface-based solutions can help in reducing and adapting to climate change by lowering air temperature. The questions of interest of the study were determined as follows:

- What is the temporal variation of LST?
- What is the temporal change in the NDVI index between 2014 -2023 and how did this change affect the LST?
- What is the temporal change in the NDBI index between 2014 - 2023 and how did this change affect the LST?
- How is the correlation between LST, NDVI and NDBI in the study area?

2. Study area

Shimla Urban, also known as Shimla City, refers to the urban area of Shimla district. It encompasses the central part of Shimla and includes the commercial, residential and administrative areas. It is located on the Southern slopes of the Himalayas and is surrounded by scenic hills and valleys. The average temperature ranges from 15 °C to 30 °C (59 °F to 86 °F). The annual average precipitation is around 1,500 millimetres (59 inches) in Shimla city. The city is located at an average elevation of approximately 2,205 meters (7,234 feet) above sea level. Shimla exhibits a ridge and spur topography, with a series of ridges and valleys extending across the landscape. The coordinates for Shimla city are approximately 31.1048° N latitude and 77.1734° E longitude.The types of forests found in Shimla city include Oak forests which primarily consisting of species like Ban Oak (*Quercus leucotrichophora*) and Moru Oak (*Quercus dilatata*). These deciduous forests contribute to the green cover and provide habitat for various floral and faunal diversity. Some areas in Shimla city have Pine forests, with species like Blue Pine (*Pinus wallichiana*) and Chir Pine (*Pinus roxburghii*). Another kind of forest is mixed forests that include a combination of coniferous and broad-leaved trees.The dominant soil type in Shimla city and its

surrounding areas is brown forest soil, also known as podzolic soil. This type of soil is typically well-drained and have a moderate to high organic matter content.

Figure 1: Location of the study area.

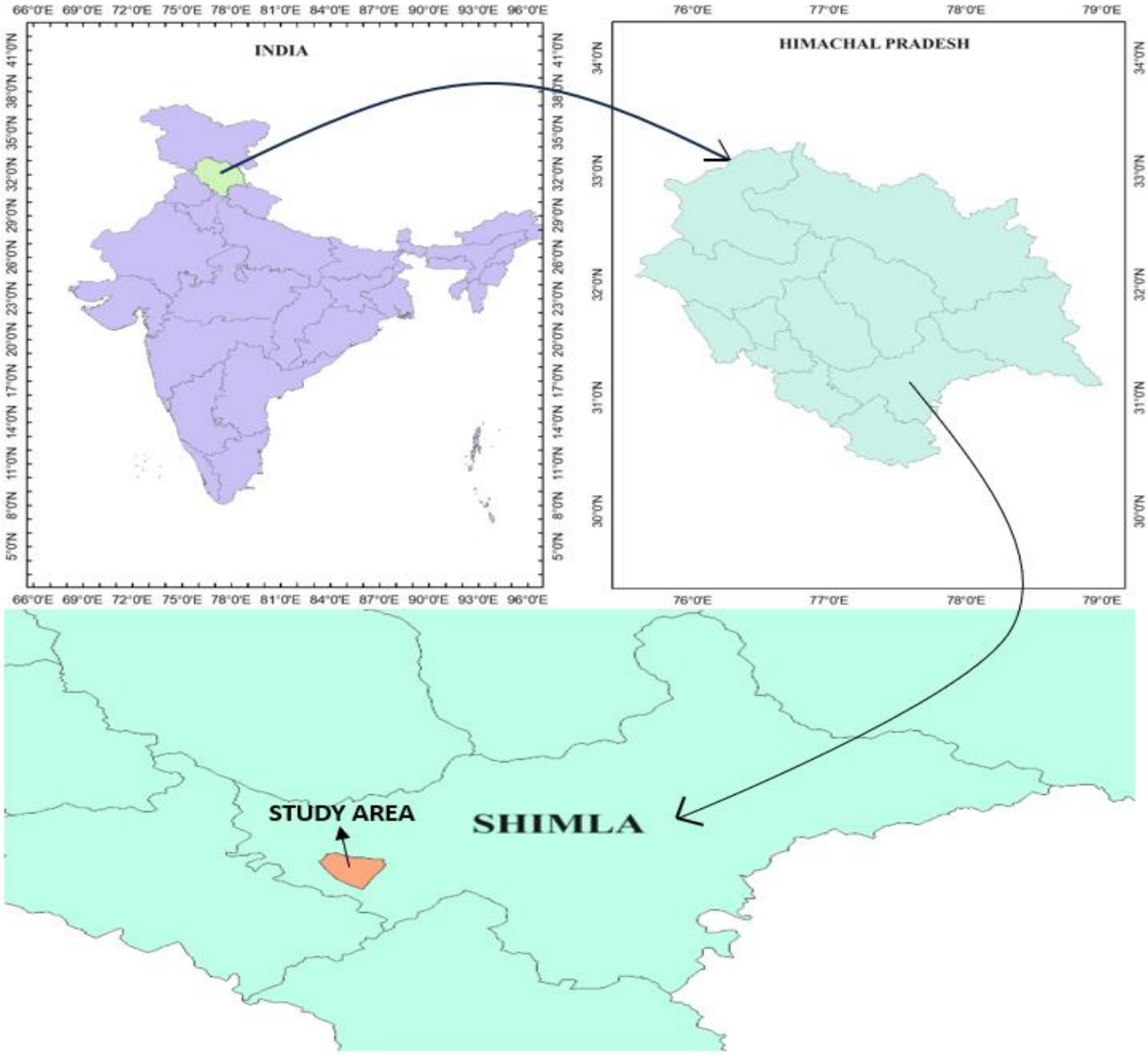

3. Methodology

3.1 Methodology for Land Surface Temperature (LST) estimation for LANSAT 8

For the estimation of land surface temperature, the raw image satellite tile for path-147 and row-039 from USGS Earth Explorer has been downloaded for the year 2014 to 2023. The images collected from satellite are introduced to geometric and radiometric modifications to rectify aberrations. Universal Transverse Mercator UTM coordinate system (WGS 1984 43N) is used to geometrize the image.

3.1.1 Conversion of Digital Numbers (DN) to Top of Atmospheric Spectral Radiance

The top of atmosphere radiance (TOA) corrects for atmospheric interference, which can distort the actual surface temperature readings. By factoring in atmospheric conditions, TOA provides more

accurate estimates of LST, enabling better understanding and monitor land surface temperatures for our study. The thermal band data (band 10 and band 11) DN is converted to TOA spectral radiance using the radiance rescaling factors provided in the metadata file.

$L_\lambda = M_L \times Q_{cal} + A_L$ (1)

Where, $L_\lambda$is the TOA spectral radiance in [(Watts/(m^2×srad×μm)], M_L is the Band-specific multiplicative rescaling factor (RADIANCE_MULT_BAND_x, from the metadata), A_L is band-specific additive rescaling factor (RADIANCE_ADD_BAND_x, from the metadata) and $Q_{cal}$is thequantized and calibrated standard product pixel values (DN).

3.1.2 Conversion of TOA to At-Satellite Brightness Temperature

Thermal band data is converted from spectral radiance to top of the atmosphere brightness temperature using the thermal constants in the MTL file as:

$$BT = \frac{K_2}{\ln\left[\left(\frac{K_1}{L_\lambda}\right)+1\right]} - 273.15 \quad (2)$$

Where, BT is the Top of atmosphere brightness temperature (K), L_λ is the TOA spectral radiance [in Watts/(m^2×srad×m)], $K_1$is band-specific thermal conversion constant(K_1_CONSTANT_BAND_x, from the metadata) and K_2 is the band-specific thermal conversion constant (K_2_CONSTANT_BAND_x, from the metadata).

3.1.3 Calculation of Normalized Difference Vegetation Index (NDVI) for the study area

NDVI values range from -1 to 1, with higher positive values indicating healthier and more abundant vegetation. This index plays a crucial role in applications like land cover monitoring, drought assessment, ecosystem health analysis, offering insights into the overall vitality and changes in vegetation over time. Red and near-infrared bands i.e., band 4 and band 5, respectively, are used for calculating the NDVI.

$$NDVI = \frac{NIR(band\ 5) - R(band\ 4)}{NIR(band\ 5) + R(band\ 4)} \quad (3)$$

Where, NIR represents the near-infrared band (Band 5) and R represents the red band (Band 4).

3.1.4 Calculation of the Proportion of Vegetation (PV) for the study area

This metric is significant in ecological and environmental studies as it helps in understanding the distribution and density of vegetation in a specific region. The proportion of vegetation PV is closely related to NDVI values for vegetation and soil. In this study, PV estimated from the NDVI traditional method is as follows:

$$PV = \left(\frac{NDVI - NDVI_{min}}{NDVI_{max} - NDVI_{min}}\right)^2 \quad (4)$$

Where, $NDVI_{max}$ and $NDVI_{min}$ are respectively the maximum and minimum NDVI that are representing NDVI of vegetation.

3.1.5 Calculation of Land Surface Emissivity for the study area

In remote sensing, accurate emissivity values are essential to ensure accurate LST calculations. Since different materials have different thermal properties, their ability to emit heat varies. It is represented by$\boldsymbol{\varepsilon}$ and formulated as:

$$\boldsymbol{\varepsilon = 0.004 \times PV + 0.986} \quad (5)$$

Where,**ε** is the Land surface emissivity, PV is the proportion of vegetation and 0.986 corresponds to correction value of the equation.

3.1.6 Calculation of Land Surface Temperature of the study area

It provides insights into the heat radiating from the land's topmost layer, reflecting the thermal conditions of various surfaces like soil, vegetation, water bodies and built-up areas. LST is a valuable parameter for understanding environmental changes, urban heat islands and agricultural dynamics.LST or the emissivity corrected land surface temperature is computed by using the equation as follows:

$$LST = \frac{BT}{1+\left[\left(\frac{\lambda BT}{\rho}\right)\ln\varepsilon\right]} \quad (6)$$

Where,LST is the Land Surface Temperature, BT stands for Brightness Temperature, λ is the wavelength of emitted radiance (10.85), **ε**is the Land surface emissivity, h is the Planck's constant (6.626×10^{-34} J s), c is the velocity of light (2.998×10^{8}m/s) and σis the Boltzmann constant (1.38×10^{-23}J/K).

3.2 Calculation of Normalized Difference Build-up Index (NDBI) for the study area

The Normalized Difference Built-Up Index (NDBI) is a remote sensing index used to detect and quantify the extent of built-up or urban areas within satellite imagery.To calculate NDBI, we used the SWIR (short-wave infrared) and the NIR (near-infrared) bands.

$$NDBI = \frac{MIR(band\ 6)-NIR(band\ 5)}{MIR(band\ 6)+NIR(band\ 5)} \quad (7)$$

Where,MIR represents middle infrared reflectance (band 6) and NIR represents the near-infrared band (band 5).

3.3 Methodology for calculation of correlation coefficient using Karl Pearson's method

The correlation coefficient, calculated using Karl Pearson's method, assesses the strength and direction of a linear relationship between two variables represented by 'r,' it ranges between -1 and 1. A positive 'r' value signifies a positive correlation, while a negative 'r' indicates a negative correlation, and an 'r' value close to 0 implies a weak or no linear correlation.The Karl Pearson's correlation coefficient (r) is given as follows:

$$r = \frac{\sum dxdy}{\sqrt{\sum dx^2}\sqrt{\sum dy^2}} \quad (8)$$

Wheredx is the deviation about mean for the variable x and dy is the deviation about mean for variable y.

4. Results and discussion

4.1 Spatial Distribution and Evaluation of LST, NDVI and NDBI

4.1.1 LST Spatial Patterns

For the study period (2014-2023), we have calibrated land surface temperature (LST) with the help of brightness temperature (BT) and land surface emissivity (LSE). The results revealed that the high temperature range (30ºC to 41ºC) is associated with the urban areas & barren soil, low temperature range (18ºC to 20ºC) is associated with water bodies whereas the temperature range (21ºC to 29ºC) belongs to the vegetation areas. In agreement with existing study of [8],our study also reflects that the rate of increase in the urbanization leads to increase in the land surface temperature.

The LST statistical data for the study period (2014-2023) is shown in Table1. The highest average land surface temperature of the study area recorded in the month of May was 29.77˚C in 2021, while the lowest reported average surface temperature is 23.40˚C in 2014.

Table 1: LST Statistical Data

Year	Maximum land surface temperature (in °C)	Minimum land surface temperature (in °C)	Average land surface temperature (in °C)
2014	32.840	13.970	23.405
2015	34.655	14.207	24.431
2016	33.517	14.522	24.019
2017	38.149	16.890	27.519
2018	37.552	15.236	26.394
2019	40.960	17.611	29.285
2020	34.792	14.241	24.516
2021	39.821	19.732	29.777
2022	36.643	18.230	27.437
2023	32.071	17.860	24.965

The graphical representation of LST data was done by plotting a bar graph between land surface temperature (maximum, minimum and average temperature) with respect to the time (year). A linear trendline is formed for land surface temperature from 2014 to 2023.

Figure 2: Variation of maximum land surface temperature w.r.t time

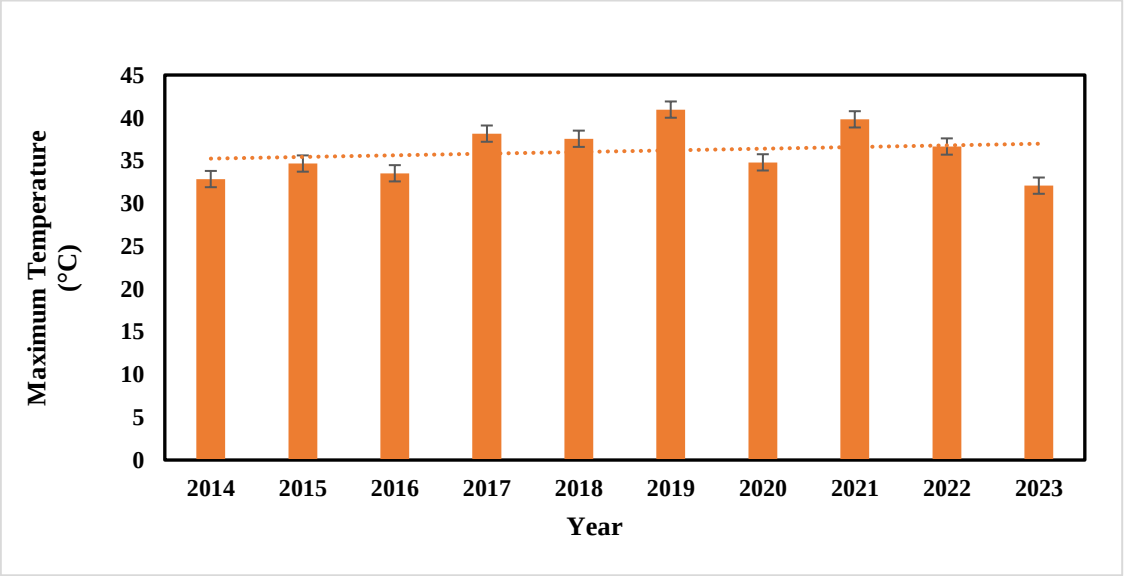

Figure 3: Variation of minimum land surface temperature w.r.t time

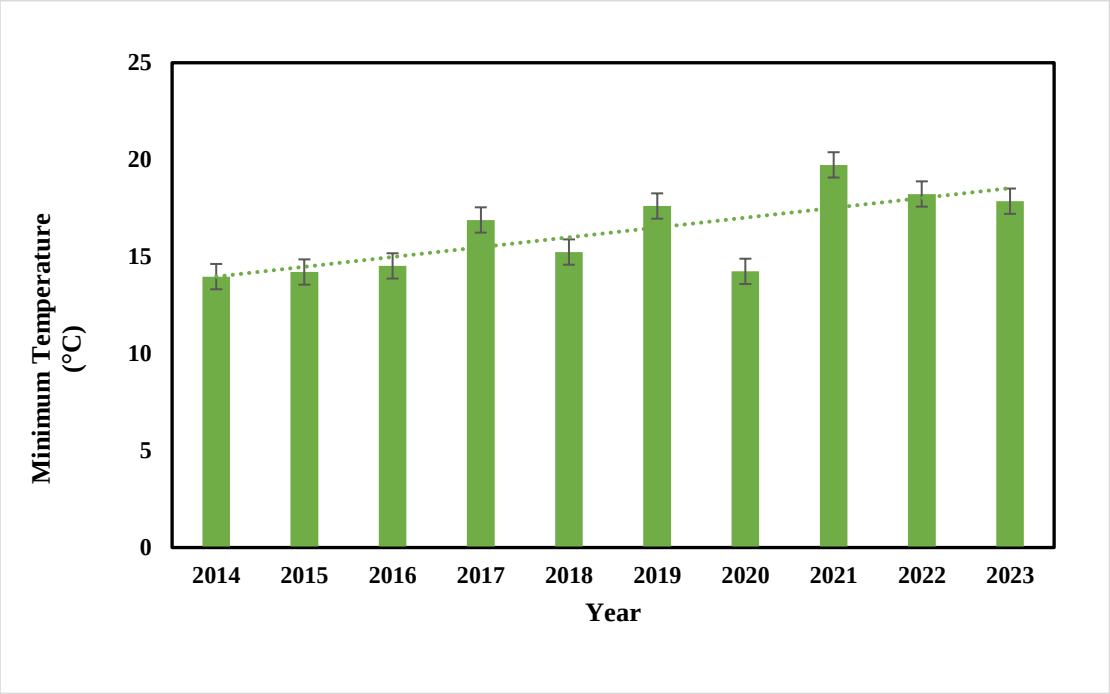

Figure 4: Variation of average land surface temperature w.r.t time

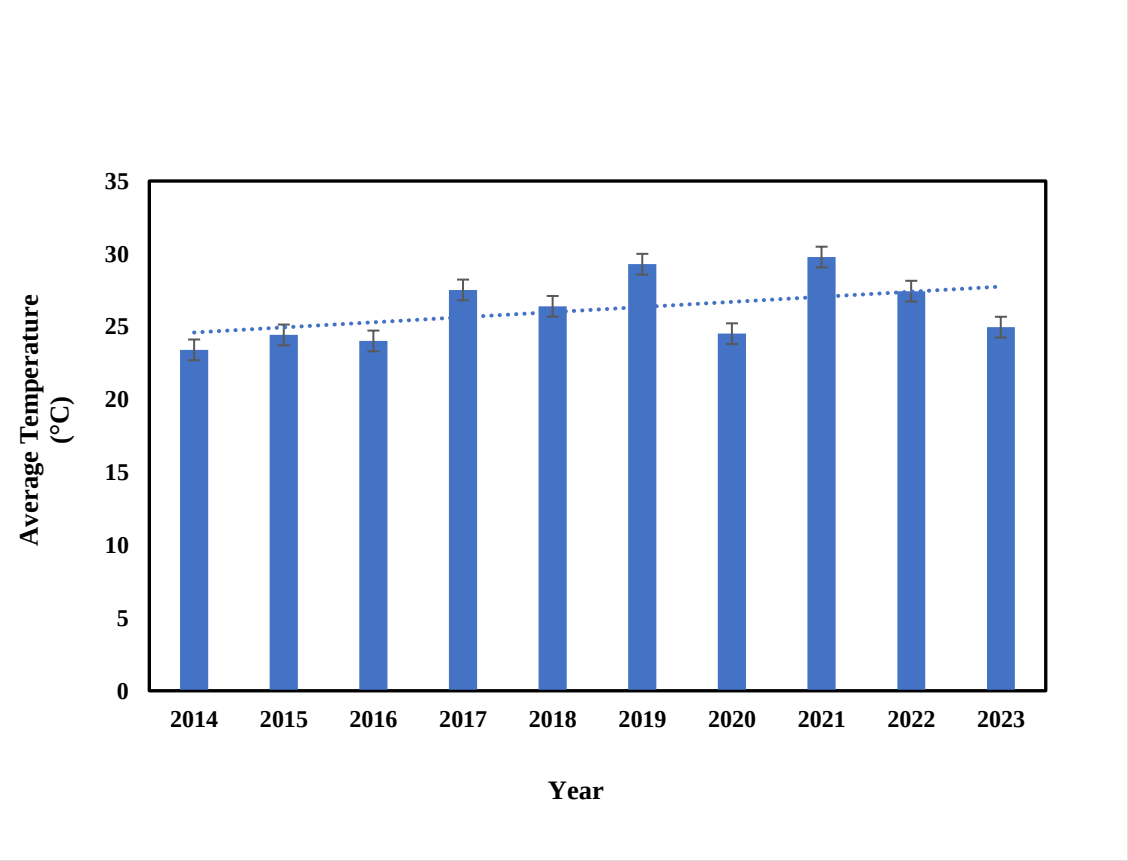

Figure 5: Comparison of the LST maps for the study area

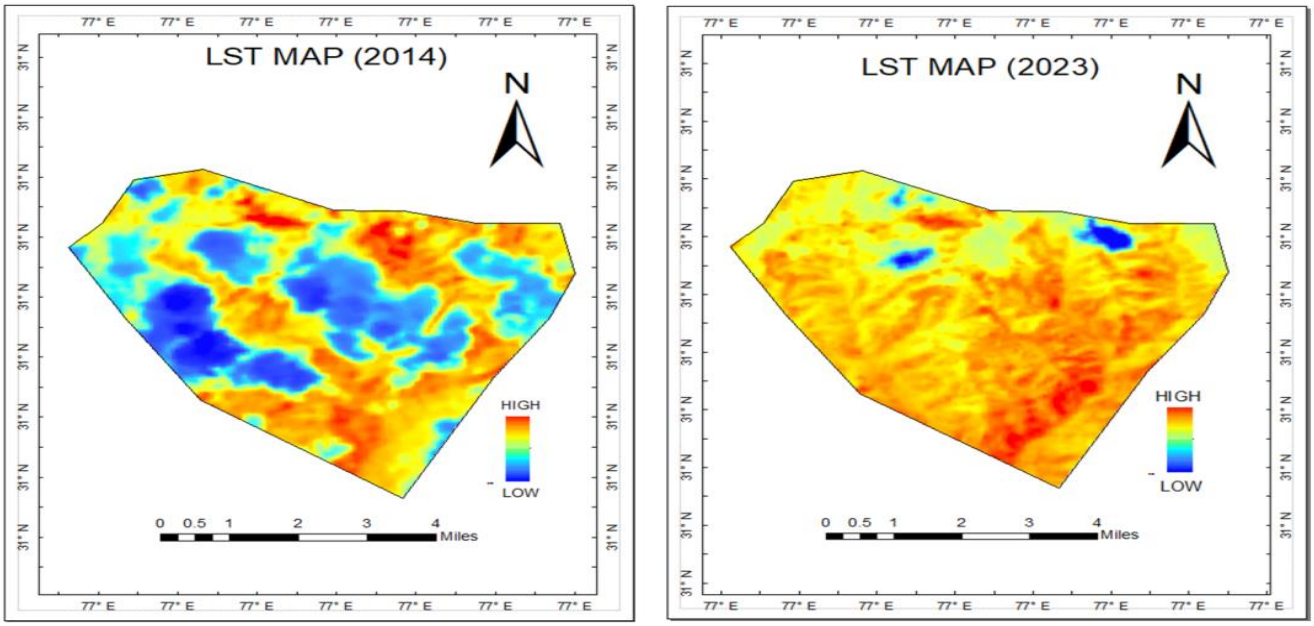

Land surface temperature is influenced by solar radiation, albedo, human activities, topography and weather conditions. Solar radiation intensity and duration, as well as albedo, affect the temperature. Human activities like urbanization, deforestation and agriculture can also affect the temperature. Topography shapes and elevations also affect solar radiation and airflow patterns. These factors result in spatial and temporal variations in land surface temperature.

4.1.2 NDVI Spatial Patterns

Normalized Difference Vegetation Index (NDVI) for the month of May during the study period (2014-2023) was calculated by using red and near-infrared bands of satellite image from the study area maps.The NDVI statistical data for the month of May is shown in the table 2,which interprets that the highest mean NDVI value 0.4898 is obtained in 2014 and lowest mean NDVI value 0.4618 is obtained in the year 2020. Higher values of NDVI represent healthier vegetation whereas low values of NDVI indicate low or stressed vegetation or the area under water body.

Table 2: NDVI Statistical Data

Year	Mean NDVI value
2014	0.4898
2015	0.4693
2016	0.4708
2017	0.4695
2018	0.4668
2019	0.4625
2020	0.4618
2021	0.4664
2022	0.4669

2023	0.4658

The result depicts the decline in NDVI of the study area and represented by figure 6. Declining value of NDVI can be attributed to the fact that urban sprawling was the major factor behind the loss of vegetation and wetland cover. Further, the low value of NDVI reflects the empty, uncultivated land areas also. For this reason, in order to better analyse the expansion of residential areas, both the parameters i.e., NDVI and NDBI are evaluated together.

Figure 6: Variation of mean NDVI w.r.t time

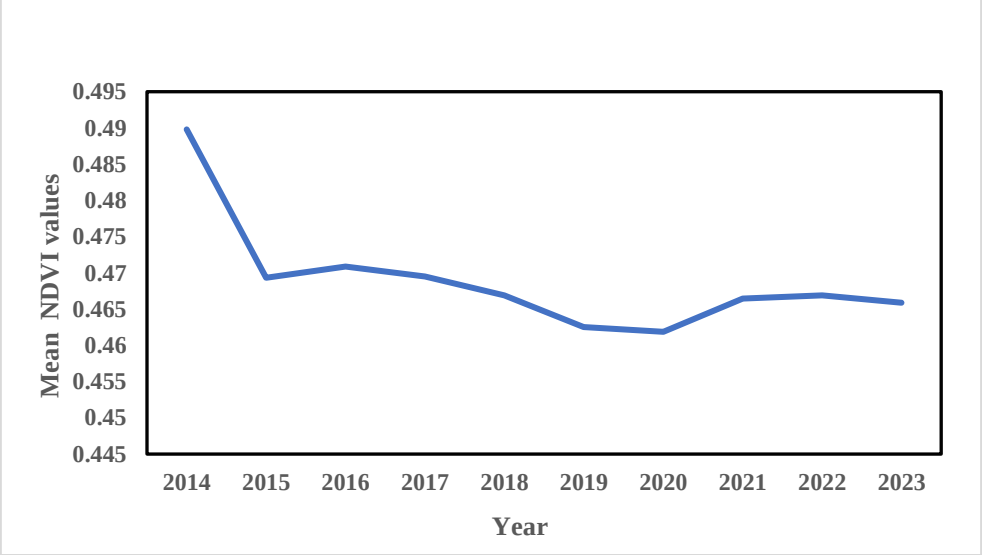

Figure 7: Comparison of the NDVI maps for the study area

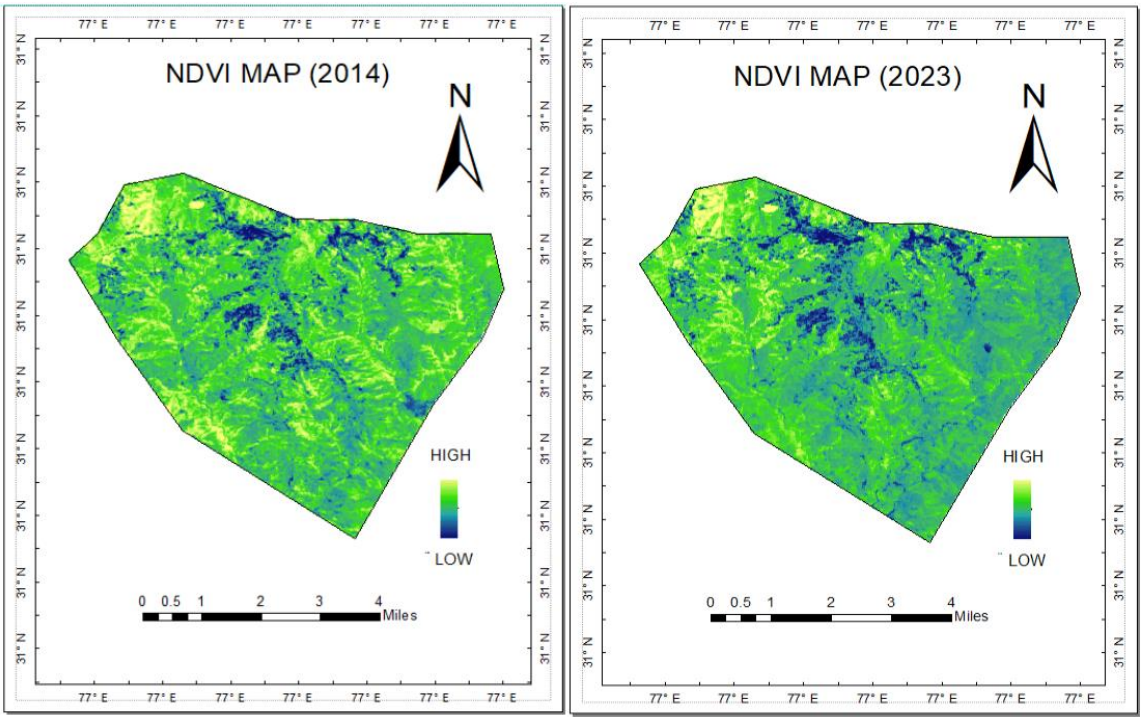

4.1.3 NDBI Spatial Patterns

A growth in the built-up areas had been observed from 2014-2023 in the study area. The NDBI statistical data for the said period is represented in the table 3. As observed, the highest mean NDBI value is 0.2051 in the year 2023 and lowest mean NDBI value is 0.185 in the year 2014.

Table 3: NDBI Statistical Data

Year	Mean NDBI value
2014	0.1850
2015	0.1856
2016	0.1913
2017	0.1936
2018	0.2013
2019	0.2026
2020	0.2031
2021	0.2043
2022	0.2044
2023	0.2051

The result revealed that the NDBI of the study area is increasing year by year and is represented in the figure 6. Increasing NDBI value can be attributed to various factors such as urbanization, population growth, industrial development, infrastructure expansion and land-use changes. As urban areas expand, the construction of buildings, roads and other infrastructure leads to higher NDBI values.

Figure 8: Variation of mean NDBI w.r.t time

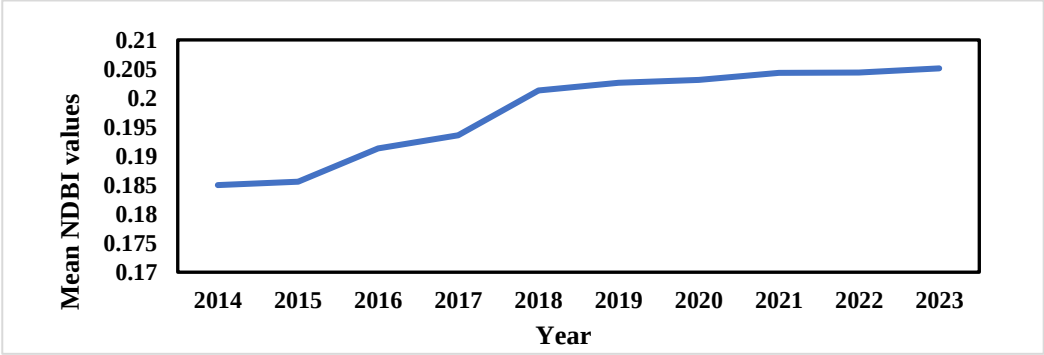

Figure 9: Comparison of the NDBI maps for the study area

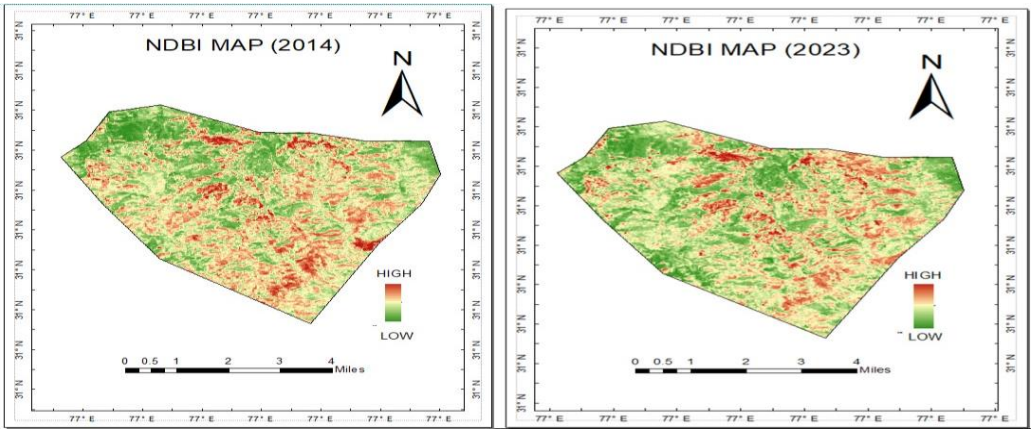

4.2 Correlation Analysis between LST, NDVI and NDBI

Correlation is the analysis used to find out the strength of the relationship between two or more variables. A correlation coefficient (r) quantifies the strength and direction of the linear relationship between two variables. The value of correlation coefficient and type of correlation is demonstrated in table 4.

Table 4: Correlation Statistical Data

Variables	Correlation coefficient 'r'	Type of correlation
LST and NDVI	r = -0.4921	Weak negative correlation
LST and NDBI	r = 0.5858	Weak positive correlation
NDVI and NDBI	r = -0.7332	Moderate negative correlation

4.2.1 LST and NDVI relationship

NDVI and LST relationship varies with season to season, but without obvious regularity. Correlation analysis has been carried out to find the relationship between LST and NDVI which have shown a weak negative correlation i.e., r = -0.4921. Our findings align with previous research conducted by [6], which highlighted a negative correlation between LST and NDVI, indicating that dissipating vegetation cover within the two study areas was responsible for the increase in LST. The linear correlation between NDVI vs LST is displayed in the figure 7.

Figure 10: Correlation between LST and NDVI

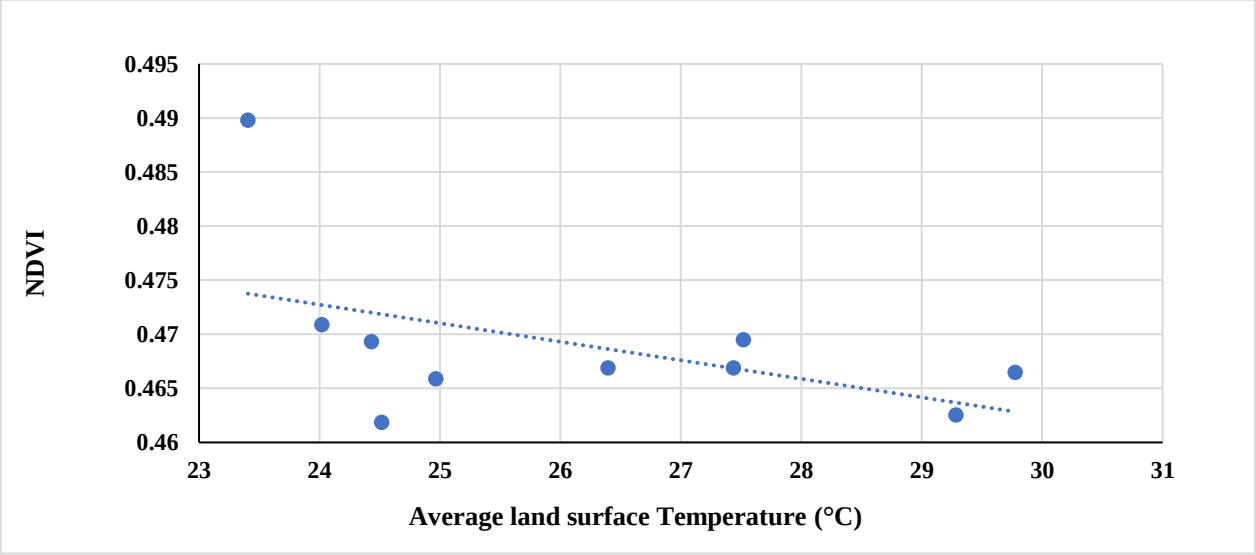

4.2.2 LST and NDBI relationship

During the study, the relationship between NDBI and LST was worked out and a positive correlation was obtained. In NDBI & LST correlation, a moderate positive correlation was obtained i.e. (r = +0.5858). The positive relationship found between NDBI and LST indicates that built-up area is generating much surface temperature variations and is the key contributor in urban heat island. The findings of [1]revealed that NDBI correlation with LST is positive which is in accordance with our study. The linear correlation of LST vs NDBI is displayed in the figure 11.

Figure 11: Correlation between LST and NDBI

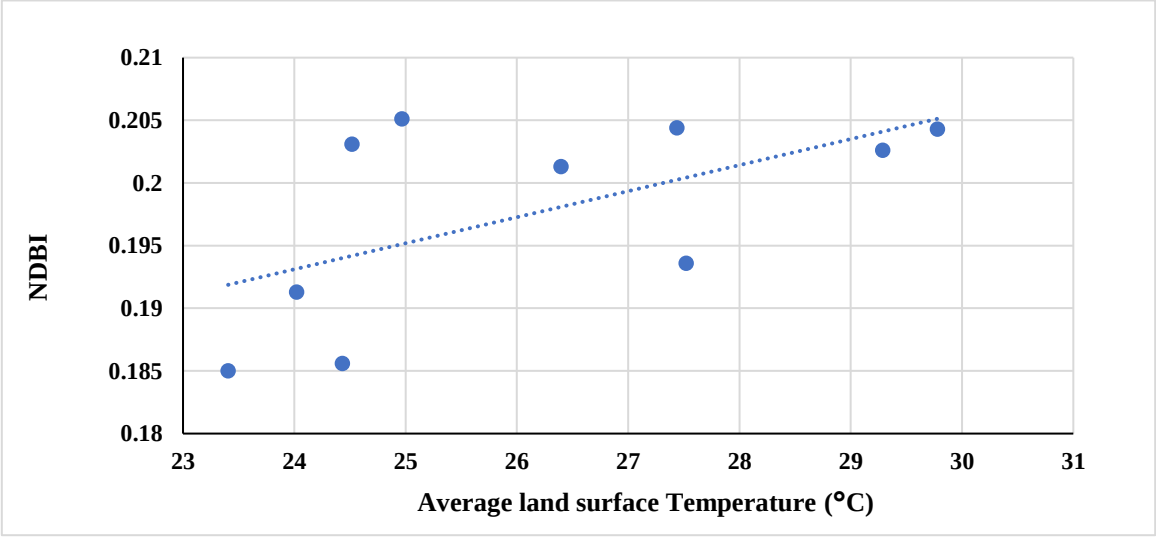

4.2.3 NDVI and NDBI relationship

Relationship between NDVI and NDBI was worked out during the study. NDVI have shown relationship with NDBI that is (r = -0.7332). [5] had computed correlation between NDVI and NDBI and a strong negative correlation was established which is in agreement with our study also.The linear correlation of NDVI vs NDBI is displayed in figure 12.

Figure 12: Correlation between NDVI and NDBI

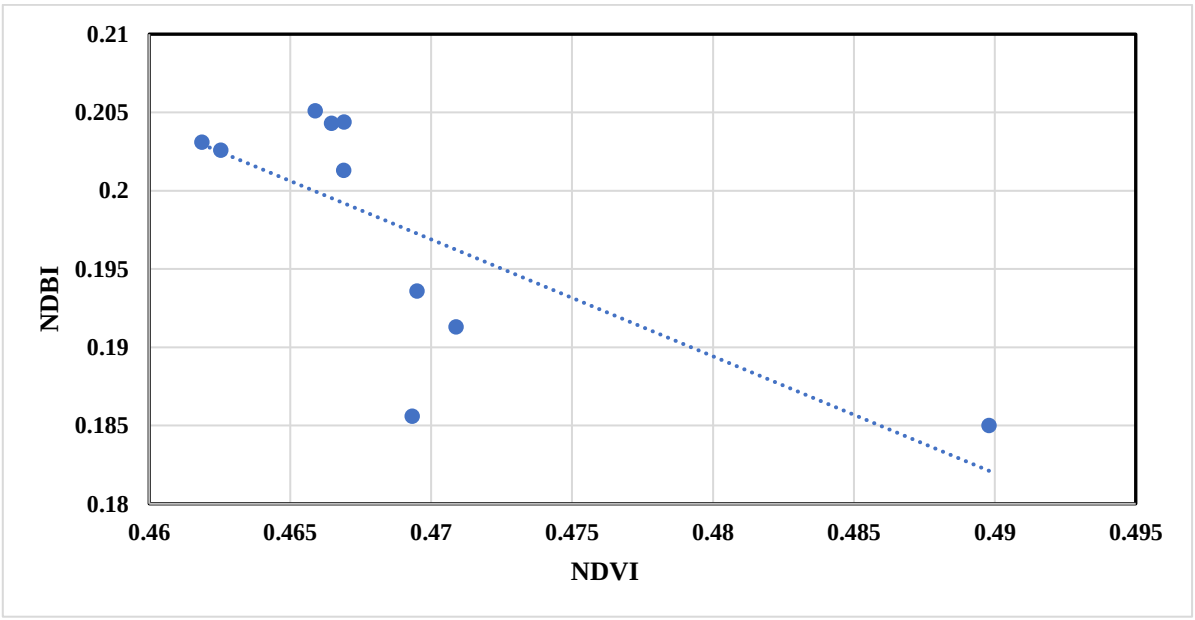

5. Conclusion

The present study monitors the LST-NDVI correlation using different Landsat satellite for a specific time interval. Thestudy clearly indicated that the intensity of LST in urban areas and barren lands is high as compared to the surrounding vegetation areas. The highest land surface temperature of Shimla city from 2014-2023 was found in the residential areas.The study showed the significant moderate positive correlation between land surface temperature (LST) and Normalized Difference Vegetation Index

(NDBI). This confirmed the strong influence of urbanization on the increment of land surface temperature in the Shimla city.The negative weak correlation between LST and NDVI reflects that green cover can mitigate the issue of increase in land surface temperature and urban heat island effect. The study reflected a moderate negative correlation between NDBI (Normalized Difference Built-up Index) and NDVI (Normalized Difference Vegetation Index)which suggested that the areas with higher built-up or urban density had lower vegetation cover.

6. References

1. Deepika V., Seeta M., Amit S., "Estimation of the land surface temperature using Landsat data 8 and 5: A comparative analysis of an industrial area from Rajasthan, India", International Journal of Advance Research, Ideas and Innovations in Technology, 2020, 6(2), 426-436.
2. Ebtihal T. A., "Influence of changes of land cover types on the surface temperature distribution for Al- Najaf city using remote sensing data", Journal of Advances in Physics, 11(9), 4029-4038.
3. Farideh T., Abolfazl R., "Quantitative analysis of spatial distribution of land surface temperature (LST) in relation Ecohydrological, terrain and socio- economic factors based on Landsat data in mountainous area", Advances in Space Research, 2021, 68(9), 3622-3640.
4. Md A.A.G., Ismail M., "Urban heat island and its effect on dweller of Kolkata metropolitan area using geospatial techniques", International Journal of Computer Sciences and Engineering, 2018, 6(10), 741-753.
5. Mohammad S.M., Jai P.S., Satanand M., "Relationship of LST, NDBI and NDVI using Landsat-8 data in Kandaihimmat Watershed, Hoshangabad, India", Indian Journal of Geo Marine Sciences, 2019, 48(1), 25-31.
6. Nour A., Victor A., Imre N., "Environmental impacts of urban sprawl using remote sensing indices: a case study of Amman city – the capital of Jordan", GeoJournal of Tourism and Geosites, 2023, 46(1), 304-314.
7. Paul M., Florian S., "Comparison of NDBI and NDVI as indicators of surface urban heat island effect in Landsat 8 imagery: a case study of Iasi. Present Environment and Sustainable Development, 2017, 11(2), 141-150.
8. Ramachandra T.V., Bharath H.A., Durgappa S.D., "Land Surface Temperature Analysis in an Urbanising Landscape through Multi-Resolution Data", Journal of Space Science and Technology, 2012, 1(1),1-10.
9. Rayan H.A., Diana M., "Using Landsat-8 data to explore the correlation between urban heat island and urban land uses", International Journal of Research in Engineering and Technology, 2016, 5(3), 457-466.
10. Reham R.M., Rabab H.A., Kadhim N.K., "Studying the relationship between land cover LST utilizing Landsat 8 data in Karbala governorate", International Journal of Civil Engineering and Technology, 2018, 9(11), 775-783.
11. Salem M., Mashaan H., "Impact of land use/land cover on land surface temperature and its relationship with spectral indices in Dakahlia Governorate, Egypt", International Journal of Engineering and Geoscience, 2022, 7(3), 272-282.
12. Shashi S., "Urban sprawl and other spatial planning issues in Shimla, Himachal Pradesh", Institute of Town Planners, 2011, 8, 53-66.

13. Suzana B.A.B., Biswajeet P., Usman S.L., Saleh A. “Spatial assessment of land surface temperature and land use/land cover in Langkawi Island”, Earth and Environmental Science, 2016, 37(1), 1-17.
14. Yaw A.T., Edmund C.M., John B.N., Olipa S.M., Tomas A.S., Diana B.F., Zhu H.N., Abena B. A., Jacob B.A., Judith O., Priscilla M.L., Faustina O., Valentine J., Brilliant M.P., Ronald O., Joyce M., Caroline O.A., Hermeshia J.M., “Estimation of land surface temperature from Landsat-8 OLI thermal infrared satellite data-a comparative analysis of two cities in Ghana”, Advances in Remote Sensing, 2021, 10(4), 131-149.
15. Youshui Z., Inakwu O.A.O., Chunfeng H., “Bi-temporal characterization of land surface temperature in relation to impervious surface area, NDVI and NDBI, using a sub-pixel image analysis”, International Journal of Applied Earth Observation and Geoinformation, 2009, 11(4), 256–264.